New High-Efficiency Source of Photon Pairs for Engineering Quantum Entanglement

Kaoru Sanaka, Karin Kawahara, and Takahiro Kuga

Institute of Physics, University of Tokyo at Komaba, 3-8-1 Komaba, Meguro-ku, Tokyo, 153-8902, Japan and Core Research for Evolutional Science and Technology (CREST), JST, Japan

(Received 6 December 2000)

We constructed an efficient source of photon pairs using a waveguide-type nonlinear device and performed a two-photon interference experiment with an unbalanced Michelson interferometer. As the interferometer has two arms of different lengths, photons from the short arm arrive at the detector earlier than those from the long arm. We find that the arrival time difference ($\Delta L/c$) and the time window of the coincidence counter (ΔT) are important parameters which determine the boundary between the classical and quantum regimes. Fringes of high visibility (80% $\pm$ 10%) were observed when $\Delta T < \Delta L/c$. This result is explained only by quantum theory and is clear evidence for quantum entanglement of the interferometer's optical paths.

DOI: 10.1103/PhysRevLett.86.5620 PACS numbers: 03.65.Ud, 03.67.–a, 42.50.Ar

Two-photon entanglement has attracted considerable interest for studying the nonlocal correlations of quantum theory [1–4], and many experiments have been performed [5–10]. The contradiction of local realism can be realized more clearly with multiphoton entanglement systems [11], which have been demonstrated experimentally in recent years [12]. We can expect these systems to be used for novel applications such as quantum cryptography [13] and quantum teleportation [14].

Multiphoton entanglement systems can be generated by parametric down-conversion (PDC). Since the probability of generating multiphoton-entangled systems decreases exponentially with the number of entangled photons, it becomes more difficult to conduct experiments with a large number of entangled photons [15]. One of the candidates for solving this difficulty is to make the ultrabright source of polarization-entangled photons proposed by Kwiat *et al.* [16]. The source is superior to other sources because nearly every pair of photons is polarization entangled. Since the total number of generated photon pairs is limited by the nonlinear susceptibility and phase-matching condition of a nonlinear crystal, a remarkable increase in the number of photon pairs cannot be expected if one uses bulk crystals.

This is to be compared to the drastic improvement of the efficiency to generate the photon pairs we present. Our method uses a waveguide-type nonlinear device originally developed for the second harmonic generation (SHG) by type-I quasiphase matching (QPM). By using the newly developed source of photon pairs, we then perform a two-photon interference experiment and show that photon pairs are in the entangled state for the interferometer's optical paths. Parametric down-converted photons from the nonlinear device are detected by two detectors located at the output ports of the interferometer. Because this interferometer is constructed with two optical paths of different lengths, photons from the shorter path arrive at the detector earlier than those from the longer path. When the time window of the coincidence counter is larger than the arrival time difference, all photon pairs from the interferometer can contribute the coincidence counts.

On the other hand, when the time window is smaller, only photons from short-short or long-long contribute the coincidence counts. If the path difference $L - S$ is larger than the single-photon coherence length, the single-photon interference will disappear but the two-photon interference will still be present, because one cannot know whether both photons took the long path, or both photons took the short path. Quantum theory predicts that the visibility of the two-photon interference should be 100%, while it is 50% at maximum by the classical model. We have observed a maximum visibility of 80% $\pm$ 10% in the experiment, clear evidence for entanglement.

The schematic of our experimental setup is shown in Fig. 1. Photon pairs generated by PDC are injected collinearly into one input port of an unbalanced Michelson interferometer which is constructed with optical paths S and L. The coincidence measurement between the two outputs of the interferometer shows two-photon interference. The two-photon state in the process of PDC is described as

$$|\psi_i\rangle = \int dk_1 \int dk_2\, \delta(k_p - k_1 - k_2)\Phi(k_1)\,|k_1\rangle \otimes |k_2\rangle, \tag{1}$$

where k_1, k_2, and k_p are signal, idler, and pump wave numbers, respectively. The δ function comes from the perfect phase-matching condition of the PDC, $\Phi(k)$ is the wave-packet distribution function, and its width Δk determines the coherence length of the down-conversion field as $\ell_{\mathrm{coh}} = 1/\Delta k$. Here the optical-path difference $\Delta L = L - S$ satisfies the condition

$$\Delta L \gg \ell_{\mathrm{coh}}\,. \tag{2}$$

so that single-photon interference effects are negligible. After passing through the interferometer, the two-photon state becomes

 0031-9007/01/86(24)/5620(4)$15.00

$$|\psi_f\rangle = \int dk_1 \int dk_2\, \delta(k_p - k_1 - k_2)\Phi(k_1)\,|k_A\rangle \otimes |k_B\rangle, \tag{3}$$

where $|k_A\rangle$ and $|k_B\rangle$ represent photon states at detectors D_A and D_B. These states are described by

$$|k_A\rangle = \tfrac{1}{2}[|k_{1S}\rangle + |k_{1L}\rangle + |k_{2S}\rangle + |k_{2L}\rangle], \tag{4a}$$

$$|k_B\rangle = \tfrac{1}{2}[|k_{1S}\rangle - |k_{1L}\rangle + |k_{2S}\rangle - |k_{2L}\rangle], \tag{4b}$$

where $|k_{nl}\rangle = |k_n\rangle e^{ik_n l}$. By substituting (4a) and (4b) into (3), we obtain

$$|\psi_f\rangle = \frac{1}{4}\int dk_1 \int dk_2\, \delta(k_p - k_1 - k_2)\Phi(k_1)[|k_{1S}\rangle|k_{2S}\rangle + |k_{2S}\rangle|k_{1S}\rangle - |k_{1L}\rangle|k_{2L}\rangle - |k_{2L}\rangle|k_{1L}\rangle - |k_{1S}\rangle|k_{2L}\rangle - |k_{2S}\rangle|k_{1L}\rangle + |k_{1L}\rangle|k_{2S}\rangle + |k_{2L}\rangle|k_{1S}\rangle]. \tag{5}$$

For example, $|k_{1S}\rangle|k_{2S}\rangle$ and $|k_{2S}\rangle|k_{1S}\rangle$ in (5) correspond to the photons which have followed the (S, S) path in the interferometers. The coincidence rate can be estimated to be $R_c = R_{c0}\langle\psi_f \mid \psi_f\rangle$,

$$R_c = \frac{R_{c0}}{2}\int dk_1 |\Phi(k_1)|^2 \times \left[1 - \frac{1}{2}\cos k_p \Delta L - \frac{1}{2}\cos(k_p - 2k_1)\Delta L\right], \tag{6}$$

when

$$\Delta T > \Delta L/c, \tag{7}$$

where ΔT is the time window of coincidence counter. Because ΔL is greater than the first-order coherence length of the wave packets, the last term in (6) will vanish and we have

$$R_c \simeq \frac{R_{c0}}{2}\int dk_1\, |\Phi(k_1)|^2\left[1 - \frac{1}{2}\cos k_p \Delta L\right]. \tag{8}$$

A similar result can be derived from a classical model. The wave number k_1 and k_2 are classical random variables which are subject to the constraint that $k_p = k_1 + k_2$, where k_p is a nonrandom variable.

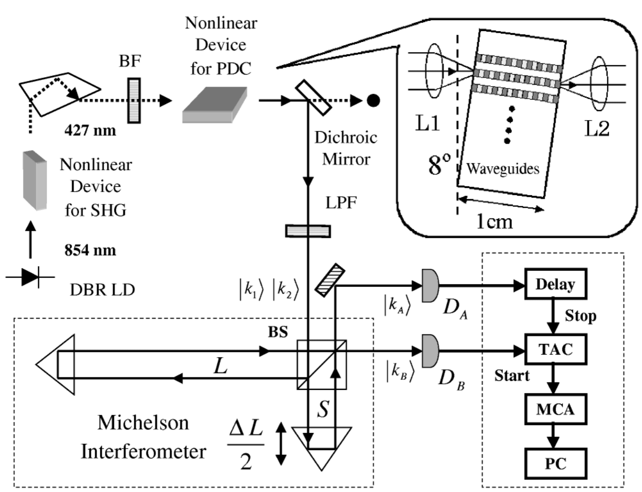

FIG. 1. Schematic of the two-photon interference experiment in an unbalanced Michelson interferometer. The path difference is set large enough such that the single-photon interference effect is nearly equal to zero.

$$\begin{aligned} R_1 &\propto \langle 1 + \cos k_1 \Delta L\rangle \simeq 1, \\ R_2 &\propto \langle 1 - \cos k_2 \Delta L\rangle \simeq 1, \\ R_c &\propto \langle (1 + \cos k_1 \Delta L)(1 - \cos k_2 \Delta L)\rangle \\ &\simeq 1 - \tfrac{1}{2}\cos k_p \Delta L. \end{aligned} \tag{9}$$

Both quantum (8) and classical (9) models predict 50% visibility. On the other hand, when the time window of coincidence counter ΔT is small enough to distinguish the path difference of interferometer

$$\Delta T < \Delta L/c, \tag{10}$$

the last four terms of (5) are not registered by the coincidence counter. In this case, the wave function that causes the coincidence becomes

$$|\psi_f\rangle = \frac{1}{4}\int dk_1 \int dk_2\, \delta(k_p - k_1 - k_2)\Phi(k_1) \times [|k_{1S}\rangle|k_{2S}\rangle + |k_{2S}\rangle|k_{1S}\rangle - |k_{1L}\rangle|k_{2L}\rangle - |k_{2L}\rangle|k_{1L}\rangle]. \tag{11}$$

Here the quantum theoretical calculation predicts the coincidence rate to be

$$R_c = \frac{R_{c0}}{4}\int dk_1\, |\Phi(k_1)|^2[1 - \cos k_p \Delta L], \tag{12}$$

and we expect fringes with 100% visibility. Two-photon interference fringes with over 50% visibility can never be explained with classical models [8,9]. Under a quasi-monochromatic wave model $k \simeq k_1 \simeq k_2$, Eq. (11) becomes

$$|\psi_{\text{entangle}}\rangle = \frac{1}{2}\int dk\, \delta(k_p - 2k)\Phi(k) \times [|k_S\rangle|k_S\rangle - |k_L\rangle|k_L\rangle]. \tag{13}$$

This means that two-photon interference with over 50% visibility reflects the two-photon entangled state of the interferometer's optical paths.

In the experimental arrangement, we utilize two waveguide-type nonlinear devices fabricated on a 1-cm-long MgO:$LiNbO_3$ substrate, one for SHG and another for generating photon pairs in the process of

PDC. The width and depth of the waveguide are 5 μm and 2.5 μm, respectively, and a domain-inverted structure was fabricated with period of 3.2 μm which satisfies the QPM condition of SHG for 850 nm. The device has high conversion efficiency, and more than 30% in SHG is reported by using a laser diode of 55 mW in power [17]. We use a cw laser beam (854 nm, 10 mW) from a distributed Bragg reflector (DBR) laser diode (SDL-5702-H1), and obtain about 0.1 mW of violet light with 1% efficiency. The coherence length of violet light is longer than the path difference of the interferometer.

After passing through a Pellin-Broca prism and a blue filter (BF), the violet light is sent to the second device. Aspheric lenses(NA = 0.4) are used for focusing violet light into the waveguide and collimating down-converted light from the waveguide. The device should be tilted by 8° from the optical axis to eliminate backreflection of the input facet of the device.

The wavelength of down-converted light is 854 nm and the bandwidth is less than 1 nm. The observed bandwidth is limited by the resolution of the spectrometer and is quite narrow to compare with that obtained in PDC by bulk crystals [18]. A detailed analysis of this phenomenon is under investigation and will be reported elsewhere. Briefly, the waveguide structure acts as a spatial filter to select a single transverse mode of down-converted light, and the down-converted light from each domain will interfere constructively with the periodic domain-inversion structure. By using these effects, we do not require narrow band filters or spatial filters used in all experiments based on the bulk nonlinear crystals.

We estimate that 10^5-s^{-1} photon pairs are generated with this weak violet light when we take into account the detection efficiency. A low pass filter (LPF) and dichroic mirrors are used to separate the violet beam.

The collinear signal and idler photon pairs are injected into an input port of a Michelson interferometer composed of a 50%-50% nonpolarizing beam splitter (BS) and retroreflectors. The optical-path difference of the interferometer is arranged about 55 cm to satisfy (2), and can be moved by a piezoelectric ceramic actuator (PZT). Two beams from the output ports of the interferometer are fed into single-photon detectors D_A and D_B (EG&G SPCM-AQR14). One signal is used for the start signal of a time-to-amplitude converter (TAC) and the other is used for the stop signal after it passes through an electrical delay line. We record the pulse height distribution with a multichannel analyzer (MCA) for 10 s, under computer control (PC).

An example of a pulse height distribution obtained with this interferometer is shown in Fig. 2. There are three distinct peaks in the figure and they correspond to photon pairs coming through (L, S), (S, S) or (L, L), and (S, L) optical paths from left to right, respectively. Because we record the time interval distribution of coincidence counts, we can analyze two-photon interference visibility with a delayed choice of the coincidence time window. In the case where we sum up all three peaks, i.e., $\Delta T = 5$ ns and the experimental condition satisfies (7), the visibility of observed fringes should be less than 50% (classical regime). Figure 3(a) shows coincidence count rates as a function of the optical-path difference ΔL, while the single count rate is almost constant: $10\,000 \pm 500$ s^{-1}, then condition (2) is satisfied. The observed interference visibility of 41% ± 10% is explained by the classical theory. On the other hand, when we sum up only the central peak from the same records, i.e., $\Delta T = 1$ ns and this condition satisfies (10), the visibility of observed fringes could be more than 50% (quantum regime). The results are shown in Fig. 3(b). The observed visibility is quite high, 80% ± 10%. Because the visibility is over 50%, these results can be explained only by quantum theory, thus proving that the two-photon optical-path entangled state was created.

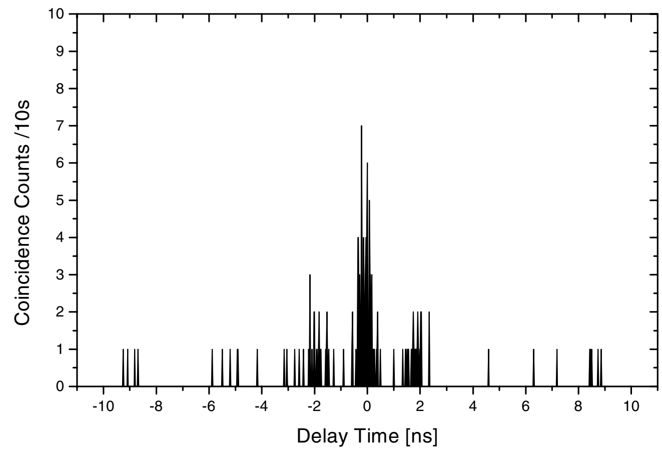

FIG. 2. Measured time difference distributions for the optical-path difference of the interferometer.

We have constructed an efficient source of photon pairs using a waveguide-type nonlinear device. The efficiency of PDC is at the same level of that obtained by bulk nonlinear crystals with about a thousand time greater pump beam [6]. We performed a two-photon interference experiment with the source of photon pairs and an unbalanced Michelson interferometer. When we sum up the region where $\Delta T > \Delta L/c$ of the record measured by a TAC, the fringe visibility is smaller than 50%, which can be explained by a classical model. On the other hand, when we sum up only the region of $\Delta T < \Delta L/c$ from the same records, the observed visibility is 80% ± 10% and clearly exceeds the classical prediction (50%). These results can be explained only by quantum theory, and is clear evidence for quantum entanglement of the interferometer's optical paths.

We can also construct an efficient source of polarization-entangled photon pairs using two waveguide-type nonlinear devices [16]. We have to take care of longitudinal walkoff of photon pairs because of the phase velocity difference between horizontal and vertical polarization photons. When one uses bulk crystals, the diameter of the

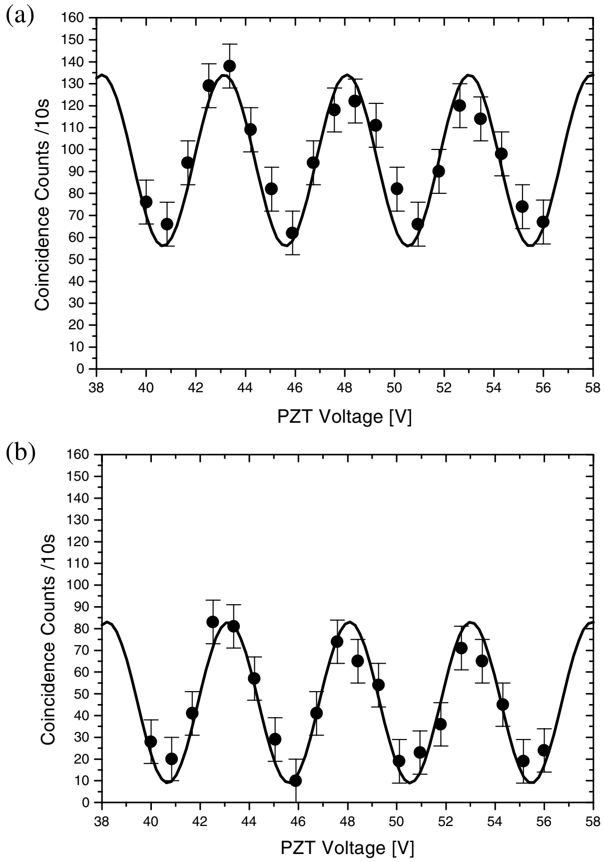

FIG. 3. Second-order interference fringes (1 V = 46 ± 8 nm). (a) Observed coincidences with 5-ns time window (circles). The solid curve is a best fit, with visibility 41% ± 10%. (b) Observed coincidences with 1-ns time window (circles). The solid curve is a best fit, with visibility 80% ± 10%.

pump light and the length of the crystal affect the indistinguishability of entangled photon pairs. However, we do not need to consider these parameters, because photon pairs exist only in a single-transverse mode of the waveguide. Our device has a great advantage over conventional bulk crystals.

The high efficiency of this source can be used for experiments which require a lot of photon pairs (quantum cryptography and quantum teleportation), and makes it possible to more efficiently generate multiphoton entanglement, which should lead to progress in quantum information technology.

We are grateful to the members of the Optical Disk Systems Development Center at Matsushita Electric Industrial Company for their experimental cooperation. This work was supported by the Matsuo Foundation and the Research Foundation for Opto-Science and Technology.

[1] A. Einstein, B. Podolsky, and N. Rosen, Phys. Rev. **47**, 777 (1935).
[2] J. S. Bell, Physics (Long Island City, N.Y.) **1**, 195 (1964).
[3] J. F. Clauser, M. A. Horne, A. Shimony, and R. A. Holt, Phys. Rev. Lett. **23**, 880 (1969).
[4] J. D. Franson, Phys. Rev. Lett. **62**, 2205 (1989).
[5] Z. Y. Ou and L. Mandel, Phys. Rev. Lett. **61**, 50 (1988).
[6] Y. H. Shih and C. O. Alley, Phys. Rev. Lett. **61**, 2921 (1988).
[7] P. G. Kwiat, W. A. Vareka, C. K. Hong, H. Nathel, and R. Y. Chiao, Phys. Rev. A **41**, 2910 (1990).
[8] Y. H. Shih, A. V. Sergienko, and M. H. Rubin, Phys. Rev. A **47**, 1288 (1993).
[9] Y. H. Shih, A. V. Sergienko, M. H. Rubin, T. E. Kiess, and C. O. Alley, Phys. Rev. A **49**, 4243 (1994).
[10] W. Tittel, J. Brendel, B. Gisin, T. Herzog, H. Zbinden, and N. Gisin, Phys. Rev. A **57**, 3229 (1998).
[11] D. M. Greenberger, M. A. Hone, and A. Zeilinger, Am. J. Phys. **58**, 1131 (1990).
[12] J.-W. Pan, D. Bouwmeester, M. Daniell, H. Weinfurter, and A. Zeilinger, Nature (London) **403**, 515 (2000).
[13] A. K. Ekert, Phys. Rev. Lett. **67**, 661 (1991).
[14] C. H. Bennett and S. J. Wiesner, Phys. Rev. Lett. **69**, 2881 (1992).
[15] C. A. Sackett, D. Kielpinski, B. E. King, C. Langer, V. Meyer, C. J. Myatt, M. Rowe, Q. A. Turchette, W. M. Itano, D. J. Wineland, and C. Monroe, Nature (London) **404**, 256 (2000).
[16] P. G. Kwiat, E. Waks, A. G. White, I. Appelbaum, and P. H. Eberhard, Phys. Rev. A **60**, 773 (1999).
[17] T. Sugita, K. Mizuuchi, Y. Kitaoka, and K. Yamamoto, Opt. Lett. **24**, 1590 (1999).
[18] W. Tittel, J. Brendel, N. Gisin, and H. Zbinden, Phys. Rev. A **59**, 4150 (1999).